ELSEVIER

Kinetic and in situ infrared studies on SCR of NO with propane by silver–alumina catalyst: Role of H_2 on O_2 activation and retardation of nitrate poisoning

Ken-ichi Shimizu [*], Junji Shibata, Atsushi Satsuma

Department of Applied Chemistry, Graduate School of Engineering, Nagoya University, Chikusa-ku, Nagoya 464-8603, Japan

Abstract

The mechanistic cause of enhanced C_3H_8-SCR activity of Ag/Al_2O_3 by H_2 addition was investigated by kinetic and in situ infrared (IR) studies. Kinetic studies found that hydrogen addition results in decreased activation energy for NO reduction (from 224 to 61 kJ mol^{-1}), decreased reaction orders with respect to O_2 (from 1.38 to 0.01) and C_3H_8 (from 1.91 to 0.76), and increased order with respect to NO (from -2.53 to 0.49). The essential role of H_2 is in the reductive activation of molecular oxygen into reactive oxygen species involved in the oxidative activation of C_3H_8. Addition of hydrogen can also retard nitrate poisoning by reducing nitrates and thus decreasing nitrate coverage. N_2 formation via the unsteady-state reaction of nitrates with hydrogen and NH_3 formation via the $NO + H_2$ reaction also occur, demonstrating an additional effect of hydrogen on the promotion of NO reduction under the unsteady-state and unselective conditions.
© 2006 Elsevier Inc. All rights reserved.

Keywords: Nitrogen oxides; Selective reduction; Silver alumina

1. Introduction

The selective catalytic reduction of NO by hydrocarbons (HC-SCR) in the presence of excess oxygen is a potential method of removing NO_x from lean-burn and diesel exhausts [1–4]. It is now well established that Ag/Al_2O_3 is among the most active and selective catalyst for SCR by alcohol [5] or by higher hydrocarbons [6–9] under lean-burn exhaust conditions [3]. Ag/Al_2O_3 has moderate tolerance to water and SO_2 [5–7,10]. One drawback of Ag/Al_2O_3 is its significantly low activity at low temperatures (below ca. 700 K) for SCR by light hydrocarbons, such as C_3H_8, that can be the main component of unburned hydrocarbons in lean-burn and diesel exhausts. Recently, Satokawa discovered a dramatic positive effect of H_2 addition on C_3H_8-SCR activity of Ag/Al_2O_3 at low temperatures [11]. Subsequently, several research groups have investigated the "hydrogen effect" for different catalytic systems [12–24], including SCR by higher hydrocarbons [16–18]

or by NH_3 [19] on Ag/Al_2O_3 and SCR by C_3H_8 on Ag zeolites [20–22]. Recently, several authors have investigated mechanistic causes of the hydrogen effect and have presented different proposals. Burch posited that hydrogen destroys nitrate species that are strongly adsorbed, thus poisoning the silver sites [4]. Brosius et al. [17] showed that hydrogen can promote the removal of nitrates from Ag as well as the formation of nitrates on the alumina support. We reported a series of spectroscopic studies on the hydrogen effect and proposed several possible mechanisms of the hydrogen effect on C_3H_8-SCR [12,13,20–24]. First, we proposed that hydrogen acts not as a reducing agent of NO, but rather as a promoter of the C_3H_8-SCR [12]. Second, we showed that hydrogen promotes the following redox reactions over Ag/Al_2O_3 [12,13]: (1) oxidation of NO to nitrates (adsorbed NO_2 on the catalyst surface); (2) oxidation of NO to NO_2 in the gas phase; (3) partial oxidation of C_3H_8 to acetate; (4) oxidation of C_3H_8 to CO_x; (5) reaction of nitrates with a $C_3H_8 + O_2$ mixture and subsequent formation of acetate; and (6) reaction of acetate with a $NO + O_2$ mixture. Similar conclusions were reported by Sazama et al. for the hydrogen effect in decane-SCR [18]. Thus, it can be speculated

[*] Corresponding author. Fax: +81 52 789 3193.
  E-mail address: kshimizu@apchem.nagoya-u.ac.jp (K.-i. Shimizu).

that H_2 should play an essential role in the activation of molecular oxygen, as suggested by Richter et al. [15], though there currently is no evidence confirming that the activation of molecular oxygen with hydrogen is responsible for the promotion of the steady-state NO reduction. Third, we proposed that hydrogen promotes the partial reduction of isolated Ag^+ cations to $Ag_n^{\delta+}$ clusters, which should act as more efficient catalytic sites than Ag^+ cations [14,22–24]. There are two different opinions concerning the role of Ag_n clusters: (1) Hydrogen reduces Ag^+ to Ag_n clusters, which activate oxygen, as speculated by Richter et al. [15], and (2) Ag_n clusters formed during H_2–HC-SCR do not represent the unique active sites, but hydrogen itself functions in enhancement of HC-SCR [18]. The latter opinion was supported by the finding that CO cofeeding in HC-SCR caused Ag_n cluster formation but no positive effect on de-NO_x activity [24].

Although the effect of hydrogen addition on the nature of the surface adsorbed species has been well investigated by catalytic and in situ infrared (IR) studies performed under transient conditions and under simple model reaction conditions, such as $NO + O_2$ and $HC + O_2$ reactions, the mechanistic cause of hydrogen effect needs to be discussed, taking into account the steady-state HC-SCR kinetics, though such an investigation has not yet been attempted. In addition, information on the hydrogen effect under unsteady-state condition is also useful, because the automotive catalyst should work even under unsteady-state conditions such as A/F (air–fuel ratio) switching conditions. In this paper, we report kinetic and in situ IR studies of C_3H_8-SCR on Ag/Al_2O_3 conducted to provide experimental evidence of the mechanistic causes of the hydrogen effect. We demonstrate that hydrogen enhances steady-state C_3H_8-SCR by promoting the activation of oxygen and by retarding nitrate poisoning. We also investigate N_2 formation via the reaction of nitrates with H_2 and NH_3 formation via a $NO + H_2$ reaction to demonstrate the additional role of hydrogen in reduction under unsteady-state conditions.

2. Experimental

The Ag/Al_2O_3 catalyst (Ag, 2 wt%; surface area, 251 m^2 g^{-1}) was prepared by impregnating γ-AlOOH with an aqueous solution of silver nitrate, followed by evaporation to dryness at 393 K and calcination in air at 873 K for 4 h. The catalytic test was performed in a fixed-bed flow reactor with 0.01–0.1 g of catalyst at a flow rate of 100 cm^3 min^{-1}. Typical compositions of feed gas in the absence and the in the presence of H_2 were $NO/C_3H_8/O_2/He = 0.1\%/0.2\%/10\%/$balance and $NO/C_3H_8/O_2/H_2/He = 0.1\%/0.1\%/10\%/0.5\%/$balance, respectively. Kinetic studies (e.g., determination of reaction order and apparent activation energy) were made under the conditions of NO and C_3H_8 conversions <30% by varying the amount of catalyst. The effluent gas was analysed by gas chromatography (GC) and NO_x analysis (Best BCL-100uH). The reaction rates of NO and C_3H_8 were calculated using the amounts of N_2 and CO_x (CO + CO_2) determined by GC.

In situ IR spectra were recorded on a JASCO FT/IR-620 equipped with a quartz IR cell connected to a conventional flow

reaction system, as in our previous studies [7–9,12,13,25,26]. The sample was pressed into a 0.07 g of self-supporting wafer and mounted into the quartz IR cell with CaF_2 windows. Spectra were measured accumulating 20–100 scans at a resolution of 2 cm^{-1}. A reference spectrum of the catalyst wafer in He taken at measurement temperature was subtracted from each spectrum. Before each experiment, the catalyst disk was heated in 10% O_2/He at 773 K for 1 h, followed by cooling to the desired temperature and purging for 30 min in He. Then a flow of various gas mixtures was fed at a rate of 100 cm^3 min^{-1}. Typical feed gas compositions were the same as those in the reaction experiments. The time-resolved change in the outlet concentration of reactants or products was monitored by the mass quadrupole apparatus. To prevent changes in the operating pressure of the IR cell, the excess flow from the cell was sent to vent. The quantification of the product concentration was carried out by calibrating the mass response using a calibrated mixture in He of each component.

3. Results and discussion

3.1. Effect of hydrogen on O_2 activation

Fig. 1 shows an Arrhenius plot for C_3H_8-SCR over Ag/Al_2O_3. In the absence of H_2, the rates of NO reduction to N_2 and C_3H_8 oxidation by NO_x and O_2 to CO_x gave fairly good straight lines (in a temperature range of 623–698 K), and the apparent activation energies were 224 and 229 kJ mol^{-1}, respectively (Table 1). The apparent activation energies decreased from the addition of 0.5% H_2 in the reaction gas mixture; the apparent activation energies for NO reduction and C_3H_8 oxidation were 61 and 63 kJ mol^{-1}, respectively (in a temperature range of 448–673 K). This indicates that the addition of hydrogen results in decreased activation energy of the rate-determining step or a change in the rate-determining step. The deuterium kinetic isotope effect was examined in a temperature range of 448–673 K (Table 1). The apparent activation energies in the D_2–C_3H_8-SCR reaction for NO reduction (60 kJ mol^{-1})
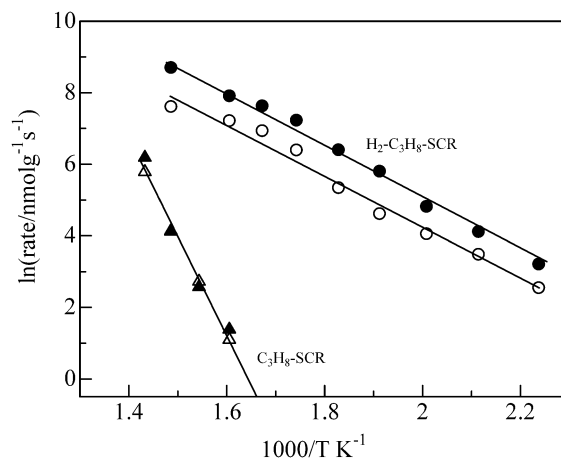
Fig. 1. Arrhenius plot for the reactions of ($\bigcirc$, $\bullet$) H_2–C_3H_8-SCR and ($\triangle$, $\blacktriangle$) C_3H_8-SCR on Ag/Al_2O_3: (open symbols) rates of NO reduction to N_2; (closed symbols) rates of C_3H_8 oxidation by NO_x and O_2 to CO_x.

Table 1
Kinetic parameters for selective reduction of NO over Ag/Al_2O_3

	C_3H_8-SCR		H_2–C_3H_8-SCR	
	NO	C_3H_8	NO	C_3H_8
E_a[a] ($kJ\,mol^{-1}$)	224 ± 5.6	229 ± 0.5	61 ± 2.5 (60 ± 0.9)[c]	63 ± 0.4 (63 ± 0.3)[c]
Order in H_2[b]	–	–	0.54 ± 0.02	0.74 ± 0.02
Order in C_3H_8[b]	1.91 ± 0.19	1.79 ± 0.32	0.76 ± 0.01	0.72 ± 0.02
Order in O_2[b]	1.38 ± 0.12	1.85 ± 0.17	0.01 ± 0.008	0.49 ± 0.01
Order in NO[b]	-2.53 ± 0.1[d]	-2.83 ± 0.02[d]	0.49 ± 0.01[e] -0.45 ± 0.01[f]	0.88 ± 0.02[e] -0.69 ± 0.01[f]

[a] Estimated from the result in Fig. 1.
[b] Estimated from the result in Figs. 2, 3, and 5.
[c] NO (0.1%)/C_3H_8 (0.1%)/O_2 (10%)/D_2 (0.5%) reaction in a temperature range of 448–673 K.
[d] NO concentration range is 200–1000 ppm.
[e] NO concentration range is 130–550 ppm.
[f] NO concentration range is 550–1000 ppm.
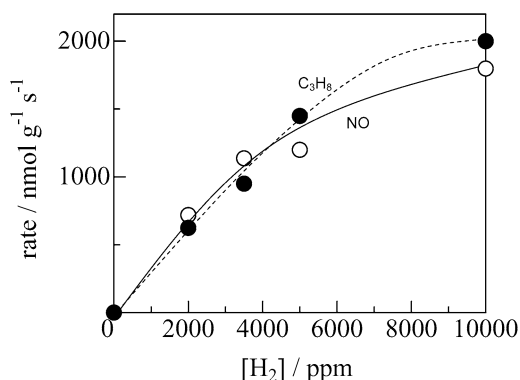
Fig. 2. Effect H_2 concentration on the rates of (○) NO reduction to N_2 and (●) C_3H_8 oxidation to CO_x for H_2–C_3H_8-SCR over Ag/Al_2O_3 at 573 K.

and C_3H_8 oxidation (63 $kJ\,mol^{-1}$) were close to those in the H_2–C_3H_8-SCR reaction, indicating that hydrogen was not involved in the rate-determining step of the H_2–C_3H_8-SCR reaction. Fig. 2 shows the effect of H_2 concentration on the NO reduction and C_3H_8 oxidation rates for C_3H_8-SCR. The rates increased with increasing H_2 concentration. As given in Table 1, the empirical reaction orders for the NO reduction and C_3H_8 oxidation (by NO_x and O_2) with respect to H_2 were 0.54 and 0.74, respectively.

Fig. 3 compares the effect of oxygen concentration on the reaction rates in the absence and presence of H_2. In the absence of H_2 (Fig. 3a), the rates of NO reduction and C_3H_8 oxidation were very low in regions of low O_2 concentration. At higher O_2 concentrations, the rates increased sharply with O_2 concentration. The empirical reaction orders estimated from the kinetic studies are listed in Table 1. The reaction orders for NO reduction and C_3H_8 oxidation with respect to O_2 in the range of 1.5–10% O_2 were 1.38 and 1.85, respectively, suggesting that O_2 activation was involved in several important steps of the NO reduction with C_3H_8. As shown in Fig. 3b, the dependence of the reaction rates on O_2 concentration in the presence of hydrogen differs significantly from that in the absence of hydrogen. The rate of NO reduction increased sharply from the addition of 1.5% O_2 and remained almost unchanged with increasing
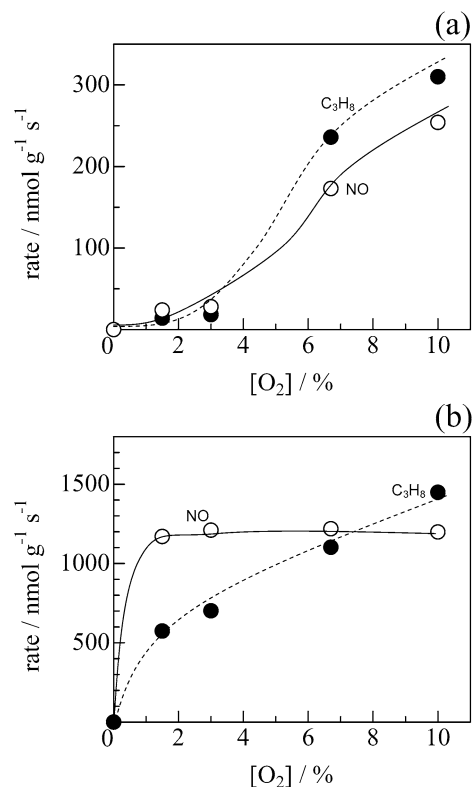
Fig. 3. Effect of O_2 concentration on the rates of (○) NO reduction to N_2 and (●) C_3H_8 oxidation to CO_x for (a) C_3H_8-SCR at 673 K and (b) H_2–C_3H_8-SCR at 573 K on Ag/Al_2O_3.

O_2 concentration. The empirical reaction orders for NO and C_3H_8 conversions with respect to O_2 in the range of 1.5–10% O_2 were 0.01 and 0.49, respectively. Taking into account the results in Fig. 1 showing that the addition of hydrogen leads to decreased activation energy of the rate-determining step or to a change in the rate-determining step, the results shown in Fig. 3 can be understood based on the assumptions that the conversion of molecular oxygen into reactive oxygen species is the rate determining-step in the absence of hydrogen, and that the activation energy for this step is decreased by the addition of hydrogen. The zero-order rate dependence on O_2 concentration (Fig. 3b) and the absence of deuterium kinetic isotope effect (Table 1) indicate that the O_2 activation by hydrogen is relatively rapid and is not involved in the rate-determining step in the H_2–C_3H_8-SCR reaction.

Fig. 4 compares the effect of C_3H_8 concentration on reaction rates in the absence and presence of H_2. In the absence of H_2, the rates of NO reduction and C_3H_8 oxidation depended strongly on C_3H_8 concentration (Fig. 4a), and these rates increased sharply at higher concentrations. The reaction orders for NO reduction and C_3H_8 oxidation with respect to C_3H_8 in the range of 200–2100 ppm C_3H_8 were 1.91 and 1.79, respectively (Table 1), suggesting that involvement of C_3H_8 activation in the important step in NO reduction. The dependence of the reaction rates on C_3H_8 concentration was significantly different in the presence of hydrogen (Fig. 4b) than in the absence of hydrogen, and the empirical reaction orders with respect to C_3H_8 for the NO reduction (0.76) and C_3H_8 oxidation (0.72) were
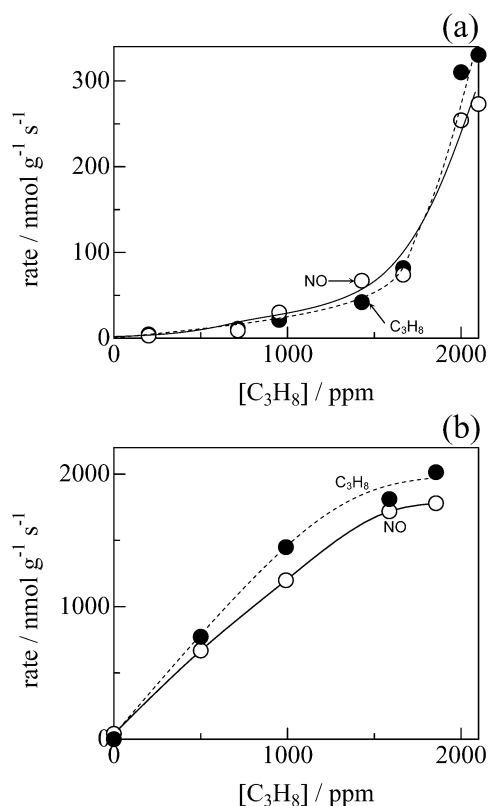
Fig. 4. Effect of C_3H_8 concentration on the rates of (○) NO reduction to N_2 and (●) C_3H_8 oxidation to CO_x for (a) C_3H_8-SCR at 673 K and (b) H_2–C_3H_8-SCR at 573 K on Ag/Al_2O_3.

Fig. 5. (○, △) NO conversion to N_2 and (●, ▲) C_3H_8 conversion to CO_x for C_3H_8-SCR on Ag/Al_2O_3 at 573 K. NO concentration is (○, ●) 200 ppm or (△, ▲) 1000 ppm.

lower than those in the absence of hydrogen. This indicates that the hydrogen addition promotes the C_3H_8-SCR reaction through the activation of reductant, C_3H_8. Previously we investigated the hydrogen effect on HC-SCR over Ag/Al_2O_3 by in situ IR spectroscopy and showed that the addition of H_2 increased the formation rate of hydrocarbon-derived oxygenate (acetate) by a factor of 190 [13]. Summarizing the above experimental results, one of hydrogen's most important roles in the promotion of C_3H_8-SCR can be described as follows. In the absence of hydrogen, activation of molecular oxygen on the surface into reactive oxygen species and subsequent oxidative C_3H_8 activation to surface oxygenates occur slowly, and either of these steps can be the rate-determining step in C_3H_8-SCR. The addition of hydrogen decreases the activation energy for the reaction of molecular oxygen into reactive oxygen species involved in the oxidative activation of C_3H_8.

The promotional effect of hydrogen in redox catalysis has also been reported from studies on the partial oxidation of hydrocarbons, including CH_4 [27–29], ethane [30], C_3H_6 [31], and benzene [32]. Wang et al. [28,30] reported that the addition of hydrogen enhanced the selective oxidation of methane or ethane by oxygen over an iron phosphate catalyst. Observing an IR band due to peroxide (O_2^{2-}) on the catalyst from adding hydrogen to the reaction mixture, these authors proposed that hydrogen, as the electron donor as well as the proton donor, reductively activates molecular oxygen [28,30]. On the other hand, it is well known that isolated Ag^+ ions in zeo-

lite are reduced by hydrogen to generate metallic or partially reduced clusters [20–22,33–35]. We reported Ag cluster formation over Ag/Al_2O_3, with in situ UV-vis results demonstrating that Ag^+ ions as the main Ag species on as-calcined Ag/Al_2O_3 were rapidly converted in a flow of O_2 (10%) + H_2 (0.5%) mixture to partially reduced $Ag_n^{\delta+}$ clusters [14]. Spectroscopic evidence on the interaction of hydrogen with partially reduced Ag_3^+ cluster in Ag–A zeolite have been well investigated by Baba et al. using ^{1}H-MAS NMR [35]. They reported that hydrogen dissociates over Ag_3^+ sites to generate acidic proton and Ag_3–H. Based on this observation, it is reasonable to assume that the addition of hydrogen results in the formation of hydride on silver clusters, which may react with oxygen to form a reactive oxidant, such as hydroperoxy radical (HO_2), peroxide (O_2^{2-}), or superoxide ions (O_2^-), as speculated by Sazma et al. [18]. The hypothetical role of hydrogen in the formation of reactive oxygen species is currently under investigation and will be reported in the near future.

3.2. Poisoning effect of nitrates

Fig. 5 shows the effect of NO concentration on the conversion of NO and C_3H_8 for C_3H_8-SCR over Ag/Al_2O_3 in the absence of hydrogen. Clearly, the activity increases with decreasing NO concentration; temperature at which NO conversion starts is about 100 K lower for 200-ppm NO than 1000-ppm NO. Note that this feature is suitable for the practical diesel de-NO_x system, in which very small concentration of NO_x must be reduced.

The reaction rates of NO and C_3H_8 for C_3H_8-SCR over Ag/Al_2O_3 at 623 K were measured as a function of NO concentration (Fig. 6a). As the NO concentration decreased from 1000 ppm to 200 ppm, the reaction rates of NO and C_3H_8 increased by a factor of 10^1–10^2. Above 200 ppm NO, empirical reaction orders for NO reduction and C_3H_8 oxidation with respect to NO showed negative values (between -2.5 and -2.8), suggesting that certain NO_x adspecies inhibit the reduction of NO by C_3H_8. Fig. 7 shows IR spectra of adsorbed species during C_3H_8-SCR over Ag/Al_2O_3 at steady state. During the reaction at 573 K, strong bands due to unidentate (1554 and
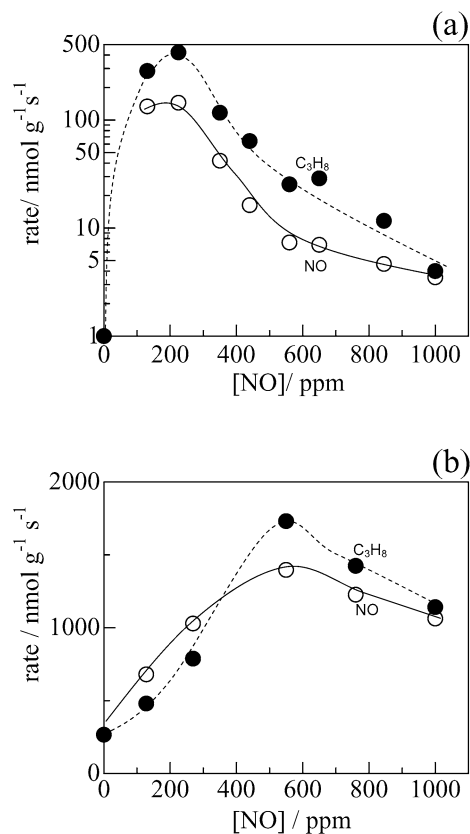
Fig. 6. Effect of NO concentration on the rates of (○) NO reduction to N_2 and (●) C_3H_8 oxidation to CO_x for (a) C_3H_8-SCR at 623 K and (b) H_2–C_3H_8-SCR at 573 K on Ag/Al_2O_3.
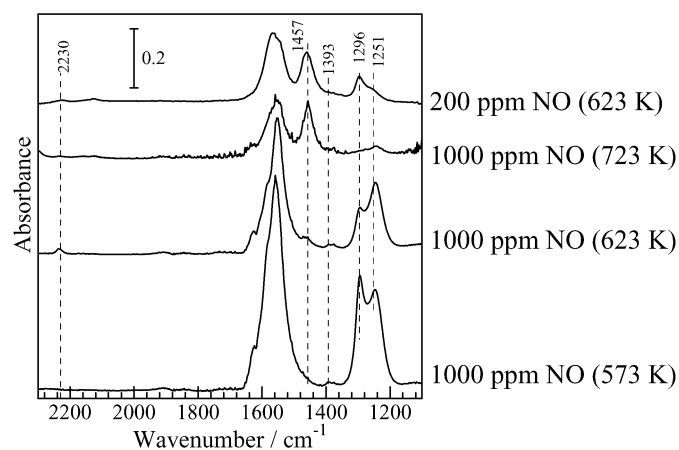
Fig. 7. IR spectra of adsorbed species during C_3H_8-SCR on Ag/Al_2O_3 in the steady states.

1292 cm^{-1}) and bidentate (1580 and 1246 cm^{-1}) nitrates [13, 25,26,36–38] were observed. The nitrate coverage depended strongly on the NO concentration in the gas phase; as the NO concentration decreased from 1000 to 200 ppm, the intensity of the bands due to nitrates (especially the bidentate nitrate) decreased. Taking into account the result that the reaction rates for NO reduction and C_3H_8 oxidation increased with decreasing NO concentration, it is evident that the nitrates adsorbed on the reaction site inhibited the adsorption and subsequent ac-
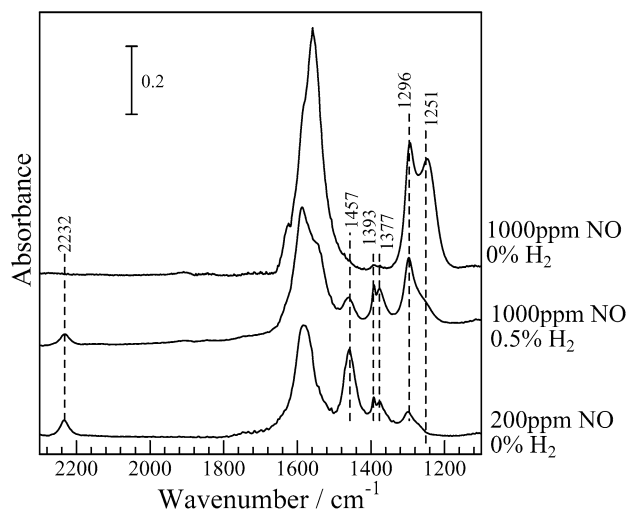
Fig. 8. IR spectra of adsorbed species during C_3H_8-SCR on Ag/Al_2O_3 in steady states at 573 K.

tivation of the reactants, resulting in decreased activity of the Ag/Al_2O_3 catalyst for C_3H_8-SCR. The IR results in Fig. 7 show that decreasing NO concentration leads to increasing intensity of the bands due to acetate (1460 cm^{-1}) [13,25,26]. This indicates that the nitrates inhibit the activation of hydrocarbon molecule. Nitrate coverage also strongly depends on temperature. Increasing reaction temperature lead to decreased intensity of the bands due to nitrates and increased intensity of the bands due to acetate (1460 cm^{-1}). As shown in Fig. 5, NO conversions increased sharply above 673 K under the condition of 1000 ppm NO. This can be understood, taking into account the result in Fig. 7, as follows. As the nitrate coverage decreases with temperature, the number of surface sites available for C_3H_8 activation increases, and thus SCR activity increases. From these results, it can be concluded that the nitrates, especially the bidentate nitrate, deactivate the Ag/Al_2O_3 catalyst for C_3H_8-SCR by strongly adsorbing on the reaction site and consequently inhibiting the adsorption and subsequent activation of C_3H_8.

3.3. Effect of hydrogen on nitrates removal

Fig. 6b plots the reaction rates for C_3H_8-SCR in the presence of hydrogen as a function of NO concentration. The NO reduction and C_3H_8 oxidation rates increased with increasing NO concentration up to 550 ppm, then decreased at higher NO concentrations. Below 550 ppm NO, empirical reaction orders for NO reduction and C_3H_8 oxidation with respect to NO were 0.49 and 0.88, respectively, whereas those at higher NO concentration (>550 ppm) exhibited negative values (−0.45 and −0.69). These results suggest that certain NO_x species were involved in the SCR reaction and that they inhibited the reaction at high NO concentration. The reaction orders with respect to NO were increased by the addition of hydrogen (Table 1), indicating that hydrogen retarded the poisoning effect of NO_x adspecies. As shown in Fig. 8, in situ IR results indicate that the addition of hydrogen to the C_3H_8-SCR reaction caused a significant decrease in the band intensity of bidentate nitrate (1580,
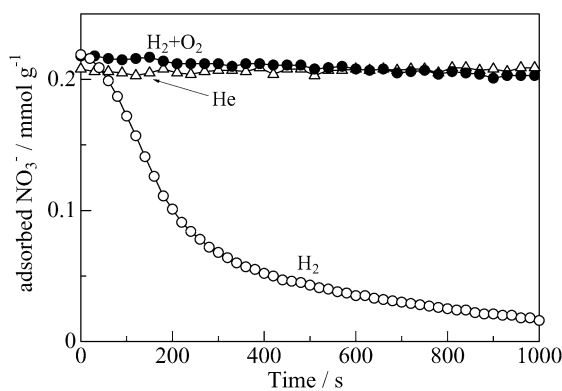
Fig. 9. Changes in the surface concentration of nitrates estimated using the integrated areas of IR band in a range 1190–1338 cm^{-1} as a function of time of exposure of Ag/Al$_2$O$_3$ to (○) H$_2$ (0.5%)/He, (●) H$_2$ (0.5%)/O$_2$ (10%)/He or (△) He at 523 K. Before the measurement, the catalyst was pre-exposed to NO (0.1%)/O$_2$ (10%)/H$_2$ (0.5%)/He for 0.5 h, followed by purging with He for 0.5 h.

Fig. 10. Changes in (○) the rate of nitrates consumption and mass intensities for (—) NO, (−··−) N$_2$, (·····) H$_2$O and (- - -) H$_2$ as a function of time of exposure of Ag/Al$_2$O$_3$ to H$_2$ (0.5%)/He at 523 K. Before the measurement, the catalyst was pre-exposed to NO (0.1%)/O$_2$ (10%)/H$_2$ (0.5%)/He for 0.5 h, followed by purging with He for 0.5 h.

1246 cm^{-1}), a relatively small decrease in the band intensity of unidentate nitrate (1554, 1292 cm^{-1}), and an increase in the band intensity of acetate. The coverage of nitrates during the H$_2$–C$_3$H$_8$-SCR reaction depended on the NO concentration in the gas phase. As the NO concentration decreased from 1000 to 200 ppm, the band intensity of nitrates, especially the bidentate nitrate, decreased. From these results, it can be concluded that the addition of hydrogen is effective in decreasing nitrate coverage on the surface and thus retarding the poisoning effect by nitrates, and that the bidentate nitrate is mainly responsible for the poisoning effect.

The dynamics of nitrate removal by hydrogen were evaluated based on the transient response of the IR spectra at 523 K (Fig. 9). The concentration of nitrates was estimated from the intensity of the bands in a range of 1180–1335 cm^{-1} due to nitrates (including unidentate and bidentate nitrates) and the extinction coefficient of nitrates (1.3 × 10^{-17} cm^{-1} cm^2 molecule^{-1}) [25]. The catalyst was first exposed to a flow of NO + O$_2$ + H$_2$ for 0.5 h to produce nitrates on the catalyst surface, followed by purging with He for 0.5 h to remove NO$_x$, O$_2$, and H$_2$ in gas-phase and weakly adsorbed species. The adsorbed nitrates were stable in a flow of He. At this time, the nitrate concentration was about 0.21 mmol g^{-1}, close to the Ag content of the sample (Ag = 0.185 mmol g^{-1}), suggesting that nitrate is adsorbed mainly on Ag$^+$ sites. The same conclusion was recently reached by Brosius et al. [17] for nitrate adsorption on an Ag/Al$_2$O$_3$ catalyst. The catalyst was exposed to a flow of H$_2$ + O$_2$ or H$_2$ while IR spectra were recorded as a function of time. The bands due to nitrates (in a range 1190–1338 cm^{-1}) decreased rapidly on exposure to H$_2$. The rate of nitrate consumption, d[NO$_3^-$]/dt, during the transient reaction of nitrates with hydrogen was determined by numerically differentiating the data in Fig. 9 and are plotted in Fig. 10. Mass spectroscopy directly connected to the in situ IR flow cell was used to provide information on the gas-phase products in the reaction of adsorbed nitrates with hydrogen. Fig. 10 includes the time dependence of mass intensities of gaseous products. Exposing the pretreated catalyst to H$_2$ produced NO and N$_2$.
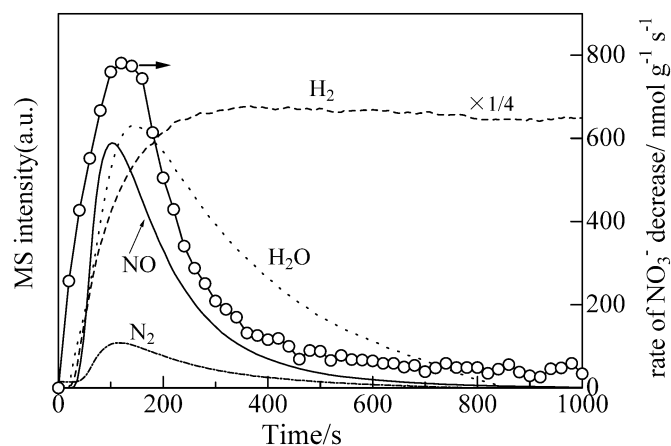
A similar experiment using a NO$_x$ analyzer for the quantification of released NO$_x$ produced a NO desorption curve similar to that determined by mass spectroscopy shown in Fig. 10 (not shown). Note that N$_2$O ($m/e = 44$) formation was negligible and that no NO$_2$ ($m/e = 46$) formation was confirmed by mass spectroscopy or NO$_x$ analysis. These results indicate that the nitrates adsorbed on the catalyst surface were reduced to mostly NO and N$_2$ through the reaction with H$_2$ as a reductant. The amounts of NO and N$_2$ estimated from the peak area in Fig. 10 were 0.13 and 0.056 mmol g^{-1}, respectively. The amount of nitrates consumed for 1000 s (0.20 mmol g^{-1}) was fairly close to that of the product, NO + 2N$_2$ (0.24 mmol g^{-1}). These results quantitatively confirm that most of the nitrates on the surface of Ag/Al$_2$O$_3$ were reduced by H$_2$ to NO and N$_2$. As Burch assumed, nitrite might be produced on the surface by the reduction of nitrates. However, no band assignable to adsorbed NO species, nitro or nitrite, was observed during this transient reaction (results not shown). We speculate that such NO adspecies may be formed but quickly desorb as NO or react with hydrogen.

3.4. NH$_3$ formation by NO + H$_2$ reaction

Fig. 11 shows IR spectra of adsorbed species during the NO + H$_2$ reaction over Ag/Al$_2$O$_3$. During the reaction at 373–673 K, bands at around 2900 and 3100 cm^{-1}, assignable to NH stretching vibration of adsorbed NH$_3$ (NH$_4^+$ or coordinated NH$_3$) [39,40], were observed, with the highest intensity at 473 K. In the NH deformation vibration region, bands assignable to NH$_4^+$ (1400, 1465, and 1690 cm^{-1}) [39,40] and those assignable to coordinated NH$_3$ (1215–1292, 1620 cm^{-1}) [39,40] were observed. As shown in Fig. 11 (spectra g and h), these bands were also observed when Ag/Al$_2$O$_3$ was exposed to a flow of NH$_3$ (0.1%)/He, confirming the foregoing band assignments. Bentrup et al. recently reported IR spectrum of adsorbed species on Ag/Al$_2$O$_3$ in a flow of NO$_2$ + H$_2$ at 573 K. The spectrum exhibited bands at 1396, 1463, and 1689 cm^{-1},
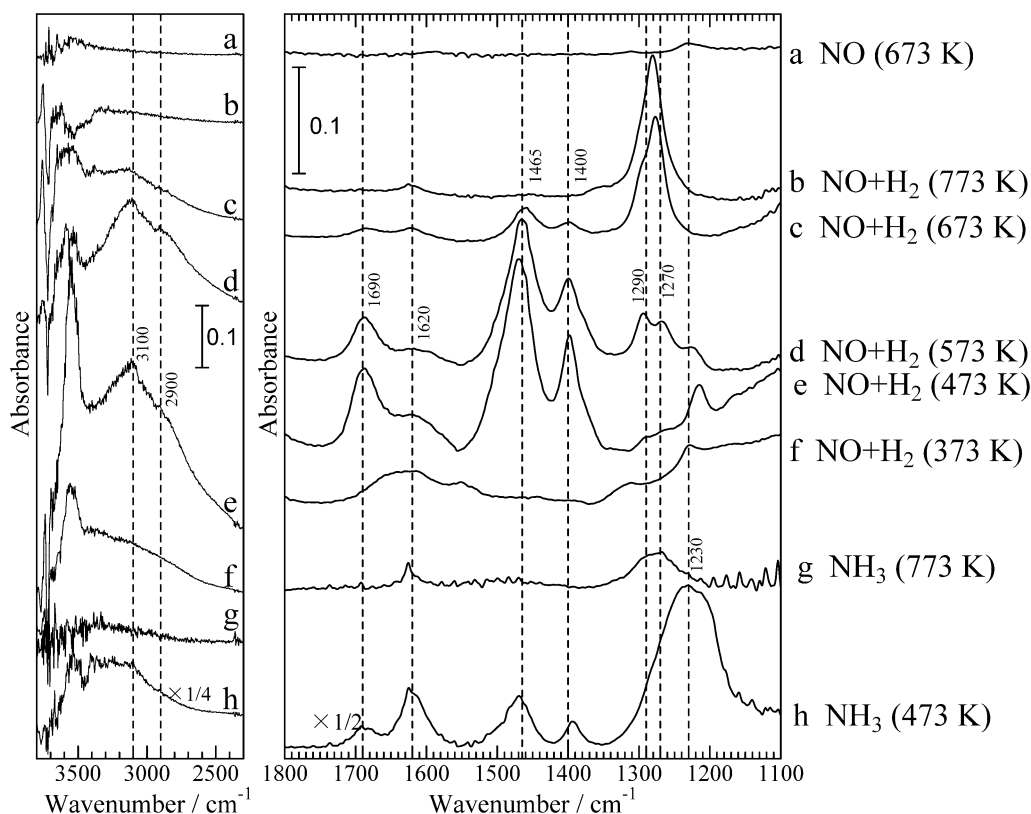
Fig. 11. IR spectra of adsorbed species in flowing (a) NO (0.4%) at 673 K, in flowing NO (0.4%)/H$_2$ (2%) at (b) 773 K, (c) 673 K, (d) 573 K, (e) 473 K, (f) 373 K and in flowing NH$_3$ (0.1%) at (g) 773 K and (h) 473 K on Ag/Al$_2$O$_3$ after flowing each gas mixture for 0.5 h.

which these authors assigned to nitro species, monodentate nitro, and adsorbed NO$_2$, respectively. Although the position of these bands are close to those of the NH$_4^+$ bands (1400, 1465, 1690 cm^{-1}) observed on Ag/Al$_2$O$_3$ during the NO + H$_2$ reaction (spectra d and e) or in flowing NH$_3$ (spectrum g), their assignments are different from ours. If these bands were assigned to nitro or NO$_2$ species, then the bands should not shift even in a flow of NO + D$_2$. But no bands were observed in the NH deformation vibration region (1200–1700 cm^{-1}) during the NO (0.4%) + D$_2$ (2%) reaction over Ag/Al$_2$O$_3$ at 473 and 773 K, demonstrating the low energy shift of all bands (result not shown). These results indicate that bands in the NH deformation vibration region (1200–1700 cm^{-1}) observed during NO + H$_2$ reaction (spectra b–g) are not assigned to nitro or NO$_2$ species. Above 473 K, the band intensity for NH$_4^+$ decreased and that for coordinated NH$_3$ increased with temperature.

Fig. 12 shows the time course of the integrated intensity of the bands due to NH$_4^+$ and coordinated NH$_3$ during the NO + H$_2$ reaction at 473 K. Formation of gas-phase NH$_3$ during the above reaction was also observed with mass spectroscopy (Fig. 12). When the flowing gas was switched to He, the band intensity for NH$_4^+$ and the mass intensity of gas-phase NH$_3$ decreased, whereas the band intensity for coordinated NH$_3$ increased. These results confirm NH$_3$ formation via the NO + H$_2$ reaction on Ag/Al$_2$O$_3$. It is established that adsorbed NH$_3$ such as NH$_4^+$ can react with NO$_2$ to produce N$_2$ [40]. Therefore,
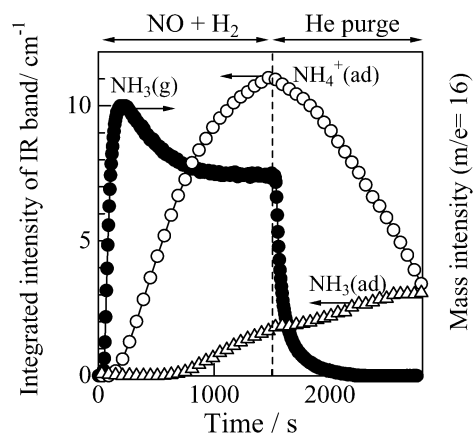
Fig. 12. Changes in the band intensities due to (○) NH$_4^+$ (in a range 1426–1520 cm^{-1}), (△) coordinated NH$_3$ (in a range 1190–1338 cm^{-1}) and (●) the mass intensity of outlet NH$_3$ as a function of time of exposure of Ag/Al$_2$O$_3$ to the NO (0.4%)/H$_2$ (2%) mixture at 473 K.

N$_2$ formation by the surface reaction of nitrates with H$_2$ can be explained as follows: Adsorbed NH$_3$ (NH$_4^+$ or coordinated NH$_3$) are produced by NO + H$_2$ reaction on Ag/Al$_2$O$_3$ and the NH$_3$ species react with nitrate (adsorbed NO$_2$) to produce N$_2$. Although this mechanism could not be an important NO reduction pathway in the steady-state HC-SCR system, it may be the main pathway under oxygen-poor conditions, such as low A/F condition in the practical automotive system.

4. Conclusion

The mechanistic cause of the hydrogen promotion effect on the activity of Ag/Al_2O_3 for C_3H_8-SCR was evaluated based on kinetic and in situ IR studies. Our findings can be summarized as follows. In the absence of hydrogen, the activation of molecular oxygen into reactive oxygen species and subsequent oxidative C_3H_8 activation to surface oxygenates occur slowly, and either of these steps can be the rate-determining step of C_3H_8-SCR. In the H_2–C_3H_8-SCR reaction, hydrogen is responsible for the reductive activation of molecular oxygen into reactive oxygen species involved in the oxidative activation of C_3H_8. In the absence of hydrogen, nitrates show a significant poisoning effect on C_3H_8-SCR. Hydrogen retards nitrate poisoning by reducing nitrates and thereby decreasing nitrate coverage. In the absence of gas-phase oxygen, N_2 is produced via the reaction of nitrates with hydrogen, probably through the formation of NH_3 on the surface by the $NO + H_2$ reaction. This may be an additional effect of hydrogen, which enhances NO reduction under unsteady-state (low A/F) condition. It is well known that the HC-SCR reaction mechanism depends strongly on the reaction condition. Consequently, we believe that the proposed role of hydrogen could explain the hydrogen promotion effect in certain reaction conditions.

Acknowledgment

References

[1] M. Iwamoto, Catal. Today 29 (1996) 29.
[2] H. Hamada, Catal. Today 22 (1994) 21.
[3] R. Burch, J.P. Breen, F.C. Meunier, Appl. Catal. B 39 (2002) 283.
[4] R. Burch, Catal. Rev. 46 (2004) 271.
[5] T. Miyadera, K. Yoshida, Chem. Lett. (1993) 1483.
[6] T. Nakatsuji, R. Yasukawa, K. Tabata, K. Ueda, M. Niwa, Appl. Catal. B 17 (1998) 333.
[7] K. Shimizu, A. Satsuma, T. Hattori, Appl. Catal. B 25 (2000) 239.
[8] K. Shimizu, J. Shibata, H. Yoshida, A. Satsuma, T. Hattori, Appl. Catal. B 30 (2001) 151.
[9] K. Shimizu, J. Shibata, A. Satsuma, T. Hattori, Phys. Chem. Chem. Phys. 3 (2001) 880.
[10] S. Satokawa, K. Yamaseki, H. Uchida, Appl. Catal. B 34 (2001) 299.
[11] S. Satokawa, Chem. Lett. (2000) 294.
[12] S. Satokawa, J. Shibata, K. Shimizu, A. Satsuma, T. Hattori, Appl. Catal. B 42 (2003) 179.
[13] J. Shibata, K. Shimizu, S. Satokawa, A. Satsuma, T. Hattori, Phys. Chem. Chem. Phys. 5 (2003) 2154.
[14] A. Satsuma, J. Shibata, A. Wada, Y. Shinozaki, T. Hattori, Stud. Surf. Sci. Catal. 145 (2002) 235.
[15] M. Richter, U. Bentrup, E. Eckelt, M. Schneider, M.-M. Pohl, R. Fricke, Appl. Catal. B 51 (2004) 261.
[16] R. Burch, J.P. Breen, C.J. Hill, B. Krutzsch, K. Konrad, E. Jobson, L. Cider, K. Eränen, F. Klingstedt, L.-E. Lindfors, Top. Catal. 30/31 (2004) 19.
[17] R. Brosius, K. Arve, M.H. Groothaert, J.A. Martens, J. Catal. 231 (2005) 344.
[18] P. Sazama, L. Capek, H. Drobna, Z. Sobalik, J. Dedecek, K. Arve, B. Wichterlova, J. Catal. 232 (2005) 302.
[19] M. Richter, R. Fricke, R. Eckelt, Catal. Lett. 94 (2004) 115.
[20] J. Shibata, K. Shimizu, Y. Takada, A. Shichi, H. Yoshida, S. Satokawa, A. Satsuma, T. Hattori, J. Catal. 222 (2004) 368.
[21] J. Shibata, Y. Takada, A. Shichi, S. Satokawa, A. Satsuma, T. Hattori, Appl. Catal. B 54 (2004) 137.
[22] J. Shibata, K. Shimizu, Y. Takada, A. Shichi, H. Yoshida, H. Yoshida, S. Satokawa, A. Satsuma, T. Hattori, J. Catal. 227 (2004) 367.
[23] U. Bentrup, M. Richter, R. Fricke, Appl. Catal. B 55 (2005) 213.
[24] B. Wichterlova, P. Sazama, J.P. Breen, R. Burch, C.J. Hill, L. Capek, Z. Sobalik, J. Catal. 235 (2005) 195.
[25] K. Shimizu, H. Kawabata, A. Satsuma, T. Hattori, J. Phys. Chem. B 103 (1999) 5240.
[26] K. Shimizu, H. Kawabata, H. Maeshima, A. Satsuma, T. Hattori, J. Phys. Chem. B 104 (2000) 2885.
[27] Y. Wang, K. Otsuka, J. Catal. 155 (1995) 256.
[28] Y. Wang, K. Otsuka, K. Ebitani, Catal. Lett. 35 (1995) 259.
[29] J.-S. Min, H. Ishige, M. Misono, N. Mizuno, J. Catal. 198 (2001) 116.
[30] Y. Wang, K. Otsuka, J. Catal. 171 (1997) 106.
[31] T. Hayashi, K. Tanaka, M. Haruta, J. Catal. 178 (1998) 566.
[32] W. Laufer, W.F. Hoelderich, Chem. Commun. (2002) 1684.
[33] M.D. Baker, G.A. Ozin, J. Godber, J. Phys. Chem. 89 (1985) 305.
[34] Y. Kim, K. Seff, J. Phys. Chem. 91 (1987) 668.
[35] T. Baba, N. Komatsu, H. Sawada, Y. Yamaguchi, T. Takahashi, H. Sugisawa, Y. Ono, Langmuir 15 (1999) 7894.
[36] N.D. Parkyns, in: J.W. Hightower (Ed.), Proc. 5th Int. Congress on Catalysis, Miami Beach, vol. 1, 1972, p. 255.
[37] F. Prinetto, G. Ghiotti, I. Nova, L. Lietti, E. Tronconi, P. Forzatti, J. Phys. Chem. B 105 (2001) 12732.
[38] A.L. Goodman, E.T. Bernard, V.H. Grassian, J. Phys. Chem. A 105 (2001) 6443.
[39] H. Knozinger, Adv. Catal. 25 (1976) 184.
[40] J. Eng, C.H. Bartholomew, J. Catal. 171 (1997) 27.